MONOTONIC AND CYCLIC UNDRAINED BEHAVIOR OF KUMAMOTO-ASO PUMICE SOIL BY TRIAXIAL AND TORSIONAL SHEAR TESTS

Muhammad Umar
The University of Tokyo

Gabriele Chiaro
University of Canterbury

16TH EUROPEAN CONFERENCE ON EARTHQUAKE ENGINEERING THESSALONIKI 18 - 21 JUNE 2018

MONOTONIC AND CYCLIC UNDRAINED BEHAVIOR OF KUMAMOTO-ASO PUMICE SOIL BY TRIAXIAL AND TORSIONAL SHEAR TESTS

Muhammad UMAR[1], Gabriele CHIARO[2], Takashi KIYOTA[3] and Hirotoshi MIYAMOTO[4]

ABSTRACT

The Kyushu Island of Japan was hit by a series of moment magnitude, M_w= 6-7 earthquakes during April 14th-16th 2016, followed by hundreds of aftershocks. The earthquakes caused a significant damage to the build and natural environment over a wide area, triggering a number of geo-disasters in the Mount Aso Caldera, comprising a large-scale flow-type slope failure known as the Takanodai landslide. The Authors conducted a series of detailed field investigations in the affected areas. Field observations indicated that the Takanodai landslide was a mobile earth slide that developed into a flow-type slide on a low angle of slope (10-15^o). In an attempt to provide insights into the failure mechanism associated with the Aso pumice soil, undisturbed and disturbed samples of volcanic soils were retrieved to be characterized in the laboratory. This paper reports on preliminary results of monotonic and cyclic undrained triaxial and large-strain torsional simple shear tests. Undisturbed sample were tested using a triaxial apparatus, while in the hollow cylindrical torsional shear device the tests were performed on reconstituted samples prepared by a special wet tamping method. The test results revealed that Aso pumice soil has the tendency to show a flow-type failure behavior characterized by an abrupt development of large shear strains when subjected to monotonic shear loadings. On the contrary, under cyclic shear stress condition, a progressive build-up of excess pore water pressure is the precursor for a flow-type failure with a rapid development of large shear strains.

Keywords: Kumamoto Earthquakes; Takanodai Landslide; Pumice soil; Triaxial test; Torsional shear test

1. INTRODUCTION

The Kumamoto earthquakes (M_w=6-7) hit the Kyushu Island of Southern Japan on April 14th-16th 2016, damaging severely houses, buildings, infrastructure, lifelines and the natural environment in Kumamoto City, Mashiki Town and in the mountainous areas of the Mount Aso Caldera (Dang et al., 2016; Mukunoki et al., 2016; Chiaro et al., 2017, among others). A large numbers of landslides were reported after the mainshock of M_w =7 that occurred on April 16th. Among many landslides, the earthquakes caused a large-scale runout slope failure in Minami Aso Village near the Aso Volcanological Laboratory of Kyoto University, Figure 1, known as the Takanodai landslide (Dang et al, 2016; Mukunoki et al., 2016) that destroyed at least 7 houses and killed 5 people, threatened many other houses and blocked several roads. Earliest field observations suggested that the key soil to cause the slope failure could be the orange-colored pumice soil deposit, Figure 2, (Mukunoki et al., 2016; Chiaro et al., 2017), hereafter referred to as Aso pumice soil. Moreover, it is the sensitivity of the pumice soil before and after the earthquake as well as the water pressure buildup could be the cause of the flow-type slope failure.

[1]PhD Student, Dept. of Civil Engineering, University of Tokyo, Japan, umar@iis.u-tokyo.ac.jp
[2]Senior Lecturer, Dept. of Civil and Natural Resources Engineering, University of Canterbury, Christchurch, New Zealand, gabriele.chiaro@canterbury.ac.nz
[3]Associate Professor, Institute of Industrial Science, University of Tokyo, Japan, kiyota@iis.u-tokyo.ac.jp
[4]Former Graduate Student, Dept. of Civil Engineering, University of Tokyo, Japan, miyamoto.hirotoshi@link-i.co.jp

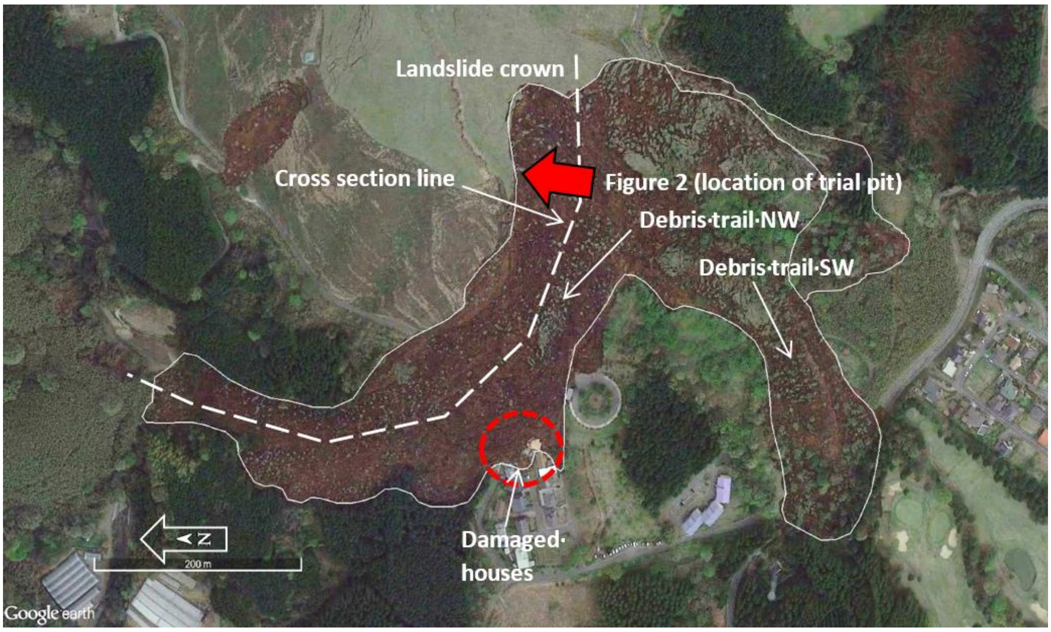

Figure 1. Google earth image of the Takanodai Landslide in Minamiaso, Kumamoto, Japan

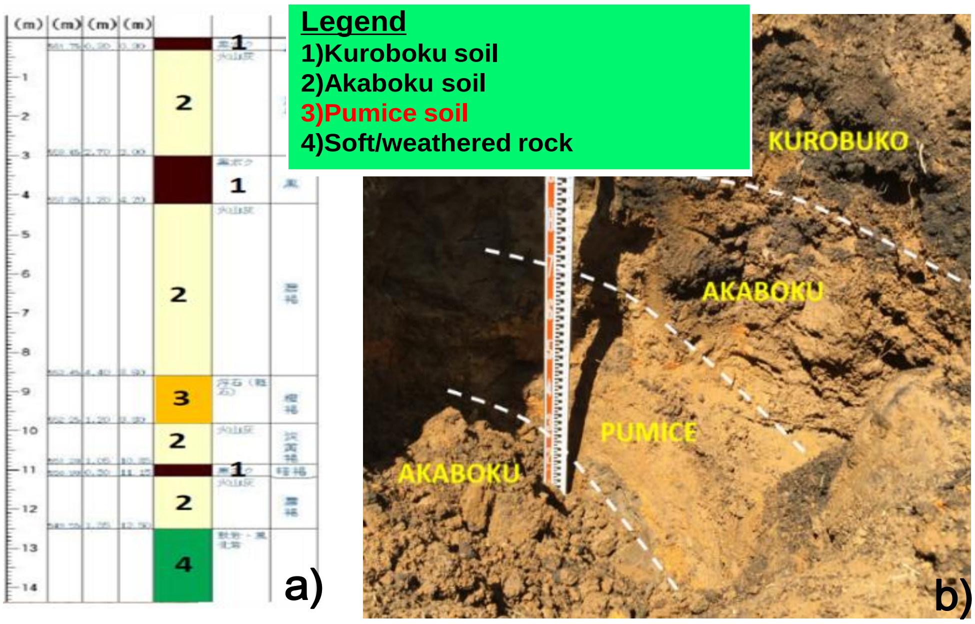

Figure 2. a) Typical soil profile at Takanodai landslide site; and b) Volcanic soils exposed in wall of a trial pit

The authors conducted a field investigation in the Mount Aso Caldera, and retrieved samples of Aso pumice soil, from the Takanodai landslide site, believed to be the key soil responsible for the activation of the landslide.

Pumice soils have a distinctive surface structure and a tendency of crushing during shearing (Liu et al. (2015); Orense, et. al (2016)). The latter was expected to affect greatly the excess pore water pressure buildup response during cyclic and monotonic shearing loading - in view of a complex volumetric response (i.e. tendency to contract or dilate under undrained shearing) of pumice – and lead the flow-type failure of pumice observed during the earthquake.

To confirm the above, in this paper, an attempt was made to characterize the undrained behavior of Aso pumice subjected to monotonic and cyclic shear loading under triaxial and simple shear conditions. In addition, the sloping condition was simulated in a torsional simple shear test to investigate the effect of the initial static shear and clarify the mechanisms for flow-type failure observed for the gentle slope in Takanodai.

2. TEST MATERIAL, APPARATUSES AND PROCEDURE

List of tests performed in this study on undisturbed and reconstituted samples is reported in Table 1. Intact and disturbed Aso pumice soil samples were collected from the Takanodai landslide investigation site. The pumice soil has a specific gravity of 2.3 (average value), an in-situ dry density of approximately 0.6 g/cm^3 and a natural water content of 117%. Its particle size distribution test and scanning electron microscope (SEM) images are shown in Figure 3. It can be observed from SEM that the particles of pumice have distinctive irregular shape and size.

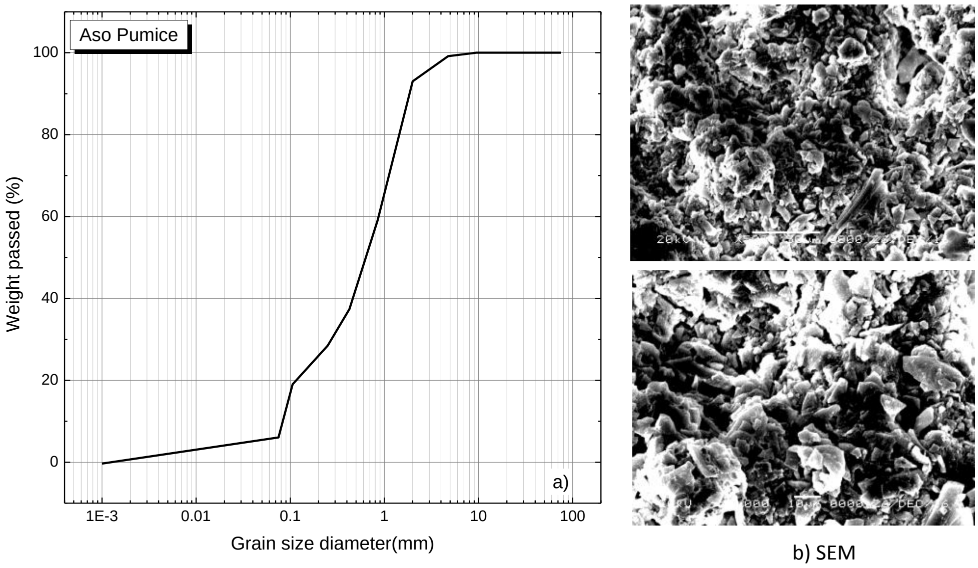

Figure 3. Aso pumice soil: a) Particle size distribution, b) SEM image analysis

Table 1. List of undrained shearing tests performed in this study

Test	Type		Dry density (g/cm^3)	Shear stresses (kPa)		Mean effective stress (kPa)
				τ_{cyclic}	τ_{static}	p_0’
ASO #1-TS	Torsional Simple Shear	Monotonic	0.56	---	0	100
ASO #2-TS			0.60	---	25*	100
ASO #3-TS		Cyclic	0.63	20	0	100
ASO #4-TS			0.58	25	0	100
ASO# 5-TX	Triaxial	Monotonic	0.52	---	0	100
ASO#6-TX		Cyclic	0.53	15	0	100
ASO#7-TX			0.56	20	0	100
* sloping ground condition						

2.1 Triaxial tests

In this study, an automated triaxial apparatus was used on cylindrical specimens of approximately 100 mm in height (H) and 50 mm in diameter (D). The axial stress was measured by means of a load cell located in the pressure chamber between the loading piston and the specimen top cap. The radial stress was measured by using a high capacity differential pressure transducer (HCDPT), while a low capacity differential pressure transducer (LDCPT) detected any volumetric change occurring during the consolidation process.
The axial strain was measured with two types of transducers: a conventional external linear variable displacement transducer (LVDT) for the small to large strains and a pair of local deformation transducers (LDTs; Goto et al., 1991) for the very small strains.

One monotonic and two cyclic liquefaction tests were carried out on undisturbed samples as shown in Table 1. Firstly, the frozen intact samples of Aso pumice were carefully extracted from the tube sampler and trimmed to a specified size (H = 100 mm, D = 50 mm) to be tested in the triaxial apparatus. To ensure a high degree of saturation (Skempton's B-value > 0.95), the double-vacuum method (Ampadu, 1991) and a back pressure of 200 kPa were applied. Undrained cyclic shearing was then applied at a strain rate of 0.02 %/min on specimens isotopically consolidated to effective mean stress (p_0') of 100 kPa that is representative of the in-situ overburden stress condition.

2.2 Torsional shear tests

An automated torsional apparatus was used to conduct a series of undrained torsional simple shear tests as shown in Figure 4, which has been developed in the Institute of Industrial Science, University of Tokyo (Kiyota et al., (2008). Such a device is capable of achieving double amplitude shear strain levels exceeding 100% by using a belt-driven torsional loading system that is connected to an AC servo motor through electro-magnetic clutches and a series of reduction gears. Torque moment and axial load are measured by a two-component load cell, which is installed inside the pressure cell. The axial load and torque moment capacities were 8 kN and 0.15 kNm, respectively. The difference in pressure levels between the cell pressure and the pore water pressure was measured by a HCDPT with a capacity of over 600 kPa. On the other hand, a LCDPT was used to measure the volume change during the consolidation process. A potentiometer with a wire and a pulley was employed to measure the rotation angle of the top cap and, thus, the large torsional deformation. Shear stress amplitude is controlled by a computer, which monitors the outputs from the load cell, computes the corresponding stress value and controls the device accordingly. It should be noted that the measured shear stress is corrected for the effects of the membrane force by using the hyperbolic equation proposed by Chiaro et al. (2015).

Four hollow cylindrical, reconstituted specimens with a dimension of 150 mm in outer diameter, 90 mm in inner diameter and 300 mm in height were tested, that were collected from the Takanodai landslide (see sampling location in Figure 1).

Similar to other volcanic soils, Aso pumice soil has a highly varying specific gravity of individual grains caused by occluded air pockets. Accordingly, conventional specimen preparation methods are not suitable for reconstituted specimen (Hyodo et al., 1998). For instance, in the case of water pluviation volcanic soils tend to segregate, with some grains floating on the water surface. Using the wet tamping method, crushing of particles may become significant. Air pluviation also has been found to be problematic. By trial and errors, in this study, the following procedure was found most appropriate to build hollow cylindrical specimens with uniform density. Precisely, to minimize the particle crushing during the specimen preparation, each specimen was prepared in 15 layers of equal height by spooning the soil (prepared at its natural water content) into the mold and subsequently applying a gentle tamping until a target density was achieved.

Due to high internal void ratio, saturation of volcanic soil requires a rigorous de-airing process (Hyodo et al., 1998; Wesley et al. 1999; Pender et al., 2006). In this study, therefore, the double vacuum method (Ampadu, 1991) was employed before and during percolation of water into the specimen. By doing so, and applying a back pressure of 200 kPa, a high degree of saturation was ensured i.e. Skempton's B-values were greater than 0.95. After completing the saturation process, the specimens were isotropically consolidated by increasing the effective mean stress state (p_0') up to 100 kPa. In the case of cyclic tests, the loading direction was reversed when the amplitude of shear stress reached the target value. Whereas, in some monotonic tests, the static shear corresponding to the in-situ sloping stress condition (i.e. shear stress component induced by slope inclination) was applied by means of drained monotonic torsional shear loading before undrained monotonic shearing (Chiaro et al., 2013).

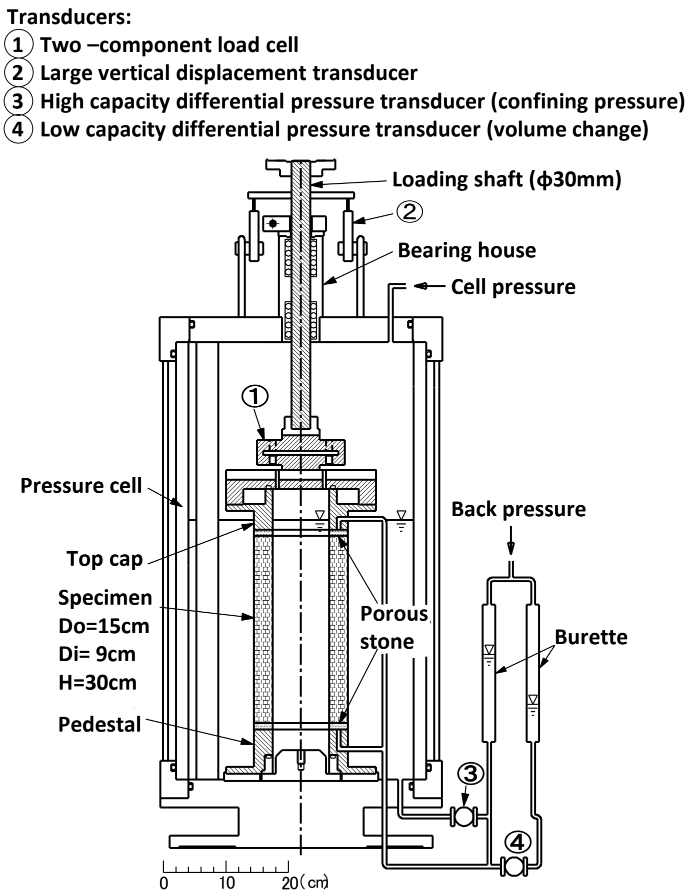

Figure 4. Torsional shear apparatus employed in this study (after Kiyota et al., 2008)

In all the tests, during the undrained shearing phase, the axial displacement of the top cap was mechanically prevented with the aim of simulating as much as possible the simple shear condition that ground undergoes during horizontal seismic excitations.

3. TEST RESULTS AND DISCUSSION

3.1 Undrained monotonic tests

Triaxial tests are usually presented in terms of deviator stress (q = (σ_1 -2σ_3)/3) and axial strain (ε_a). Whereas, torsional simple tests are presented in terms of shear stress (τ) and shear strain (γ). In this paper, for comparison, deviator stress and axial strain from triaxial tests were converted into shear stress and shear strain, respectively, using the theory of elasticity (shear stress, $\tau = 0.5*q$, and shear strain, $\gamma = 1.5*\varepsilon_a$). Figures 5 and 6 show typical results of undrained monotonic torsional shear and triaxial tests, respectively.
In both the monotonic tests, Aso pumice soil had showed a flow-type failure behavior characterized by an abrupt development of large shear strains when subjected to monotonic shear loadings. However, it can be seen from the effective stress paths, Figures 5a and 6a that the reconstituted specimen showed a purely contractive behavior, while the undisturbed specimen firstly contratced and then dilated (transition from point A to A'). In both tests, however, the post peak shear state was characterized by strain softening behavior and development of large shear strains.

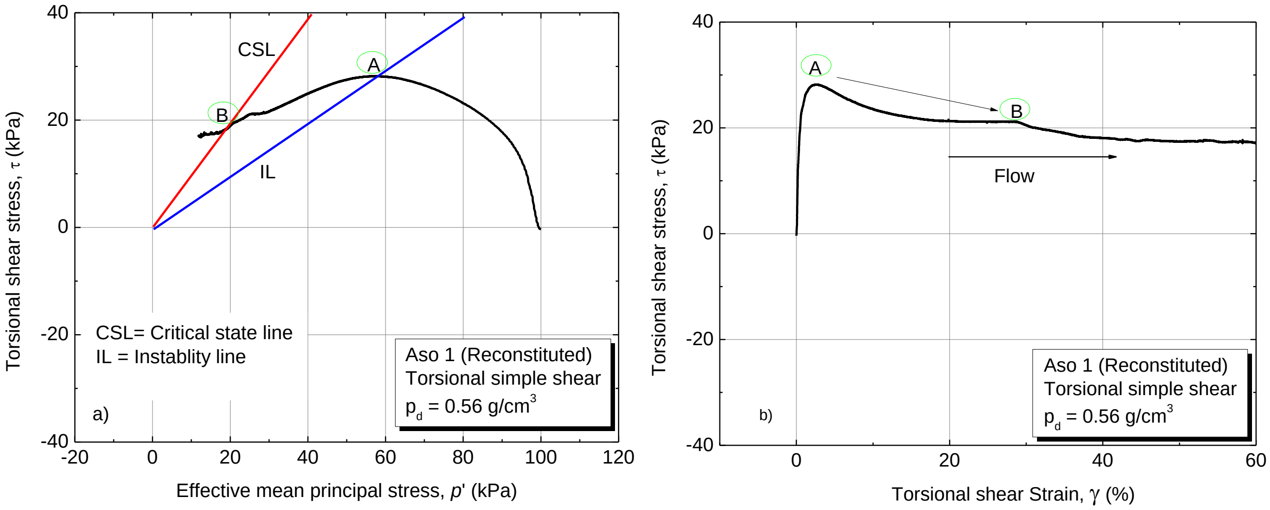

Figure 5. Torsional shear test ASO #1: a) effective stress path; and b) stress- strain relationship

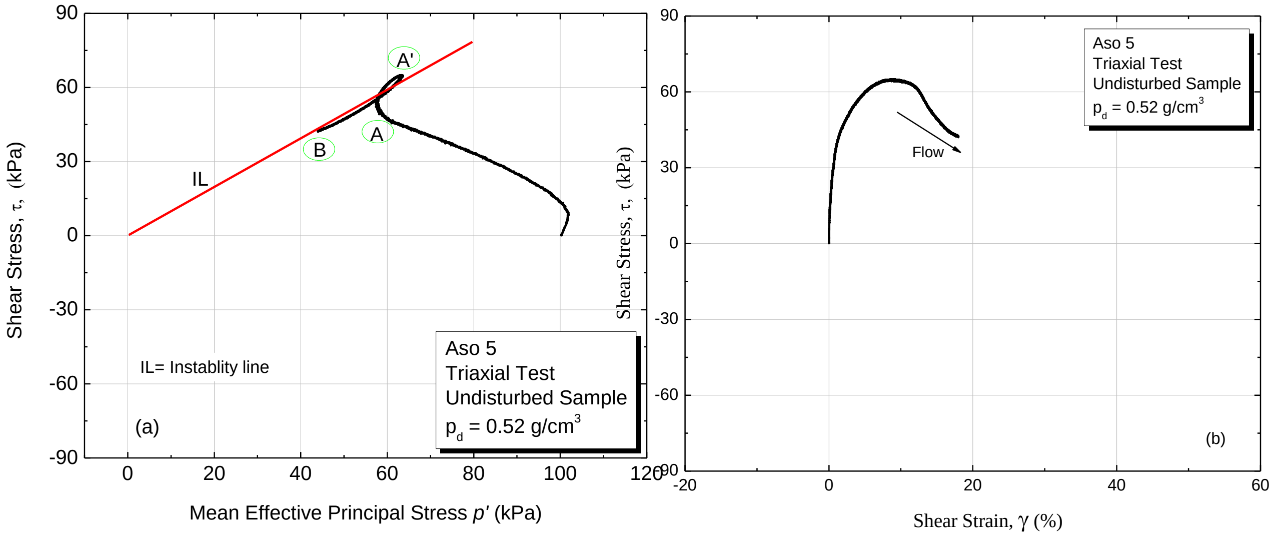

Figure 6. Triaxial test ASO #5: a) effective stress path; and b) stress-strain relationship

3.2 Undrained cyclic tests

Liquefaction (*p_0'=0*) is associated with the tendency of development of excess pore water pressure during undrained cyclic loading and consequently development of large shear strain (Kiyota et al. 2008). Figures 7 and 8 show typical undrained cyclic test results of undisturbed and reconstituted pumice specimens, respectively. The effective stress path, Figure 7a and 8a, and strain development, 7b and 8, show a contrasting behavior. In figure 7a, the applied cyclic shear stress is lower than the peak stress (i.e. point A). As a result, until the 30th cycles of shear loading, the development of shear strain is very small. However, from loading cycle 31st, the rate of development of shear strain significantly increases. Whereas, in Figure 8a, the peak stress was achieved within a half cycle and consequently the development of shear strain was immediate. Even though in both the tests the state of full liquefaction (*p_0'*=0) was not achieved, the progressive pore water pressure buildup led to a flow-type failure accompanied by an abrupt large shear strain development.

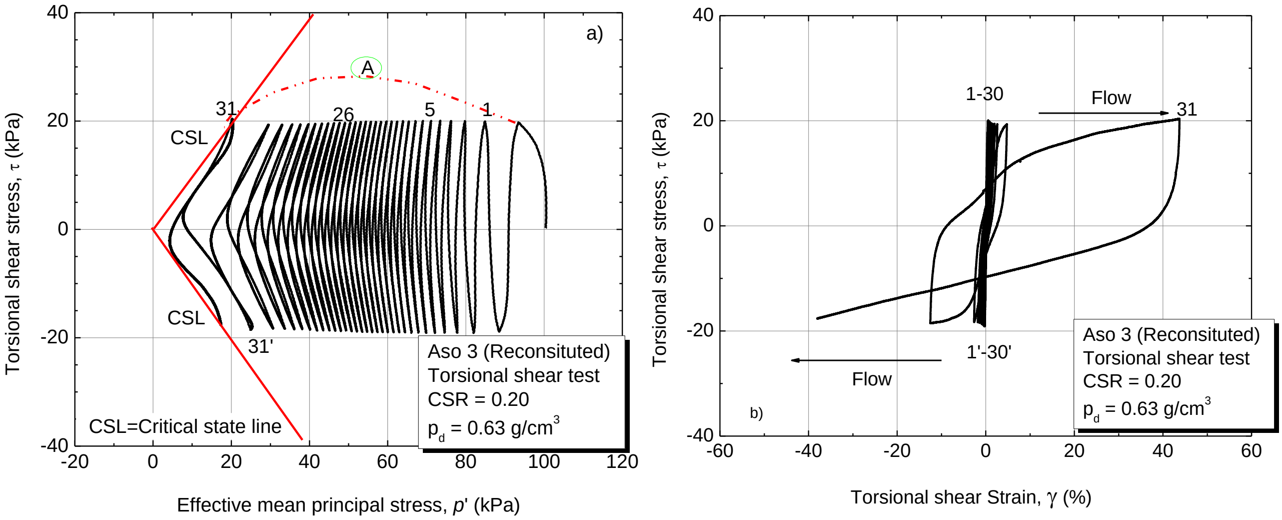

Figure 7. Torsional shear test ASO #3: a) effective stress path; and b) stress -strain relationship

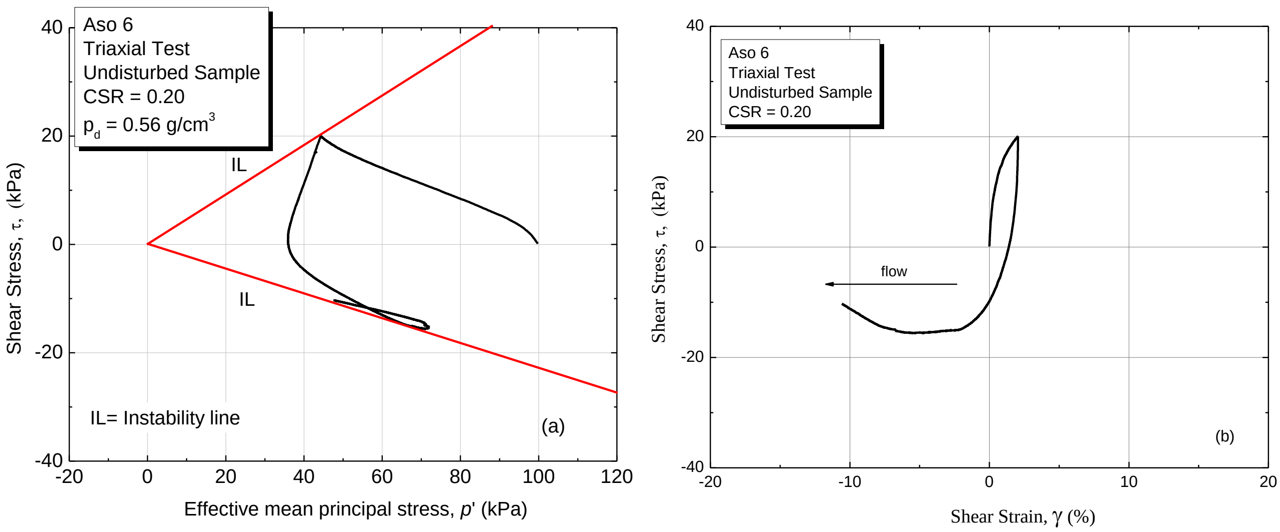

Figure 8. Triaxial test ASO #6: a) effective stress path; and b) stress-strain relationship

3.3 Comparison between Aso Pumice behavior and Toyoura sand response

To provide further insights into Aso pumice behavior, the response of Aso pumice is compared to that hard-grained Toyoura sand. Figure 9 shows the buildup of excess pore water pressure vs. shear strain development for Aso pumice and Toyoura sand under the same amplitude of cyclic stress ratio. It is evident from Figure 9b that in the case of Toyoura sand a significant increase in the rate of shear strain increment was observed only after the excess pore water pressure ratio ($r_u = u/p_0$') reached to 1 (i.e. u = p_0'= 100 kPa or full liquefaction state). While, for Aso pumice, large increment in the shear strain was observed when excess pore water pressure reached 80% or *p*' = 80 kPa, Figure 9a. Moreover, shear strain exceeding 60% was achieved without reaching the state of full liquefaction 100% buildup of excess pore water pressure.

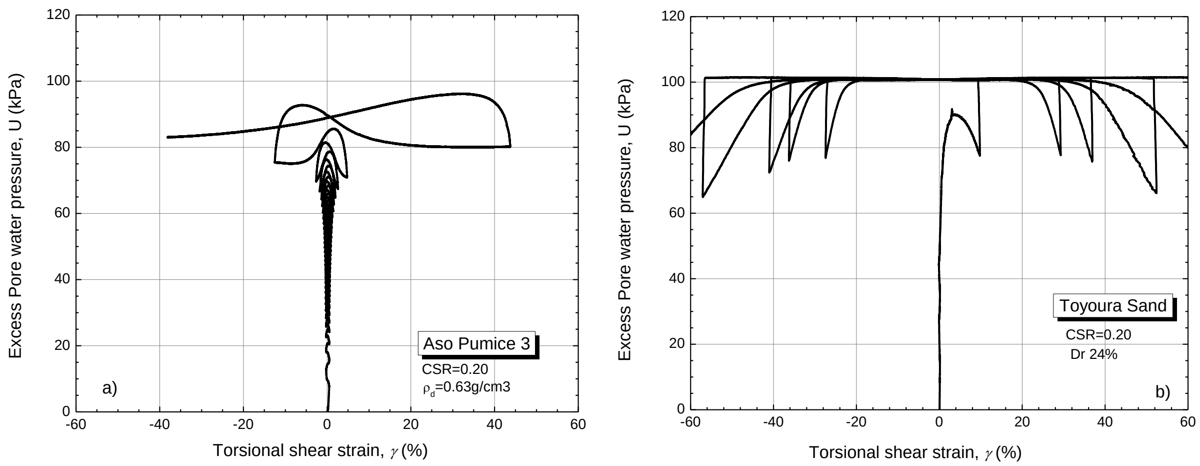

Figure 9. Pore water pressure vs. shear strain relationships from torsional shear tests: (a) Aso Pumice (Test ASO #3); and (b) Toyoura Sand

3.4 Undrained cyclic torsional shear with initial static shear

Takanodai landslide developed a flow-type slide on a low angle slope (around 10-15^o), with a travel angle from landslide crown to debris toe of approximately 6^o after the earthquake, Figure 10. To investigate the mechanism associated with development of large deformation, sloping condition were introduced in the test before applying the cyclic loading. To do so, a drained torsional pre-shearing of 25kPa was applied, which corresponds to initial static shear evaluated for the Takanodai slope.

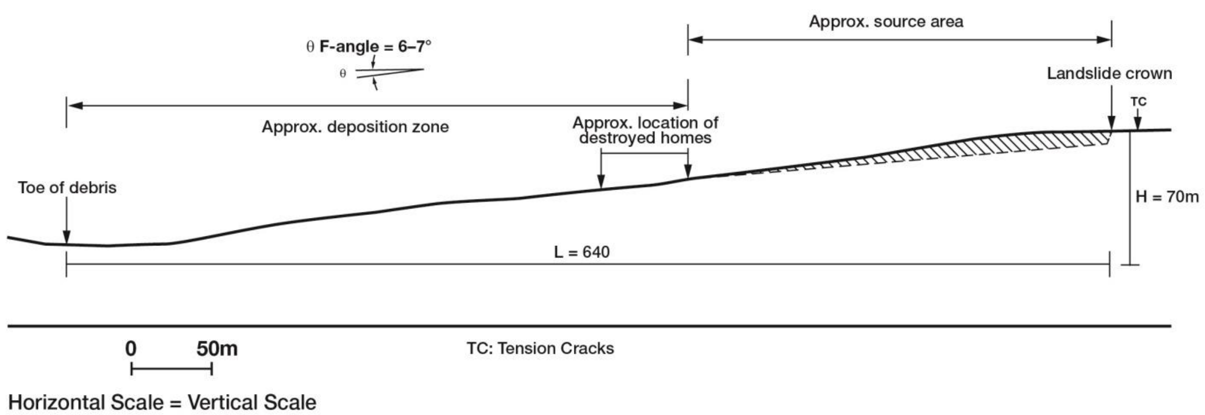

Figure 10. Cross-section A-A' through the Takanodai landslide (Chiaro et al., 2017)

Compared with the case shown in Figure 5, the overall behavior of Aso pumice soil subjected to monotonic shearing loading with initial static shear did not change significantly (Figure 11), in the sense that it remained purely contractive and strain-softening followed by large strain development was observed after the peak stress stage. However, an increase in both the undrained peak shear strength and the residual strength was observed. When compared with the response of Toyoura sand subjected to same level of static shear shown in Figure 12, it seems that Aso pumice soil behaves similarly to a loose sand specimen. However, some difference can be seen. For example, while a medium loose sand specimen usually behaves first contractive and then dilative (p' increases after reaching the phase transformation line), Aso pumice soil behaves purely contractive and the shear stress suddenly drops after reaching the failure envelop line (CSL). Therefore, a clear PTL line cannot be established for Aso pumice soil. Moreover, while after the quasi-steady stage loose sand experiences a limited strain development, Aso pumice soil undergoes large strain development. This different behavior may be attributed to: 1) the low crushability of sand particles (hard-grained material) as compared to that of Aso pumice (crushable volcanic soil); and 2) different soil structure.

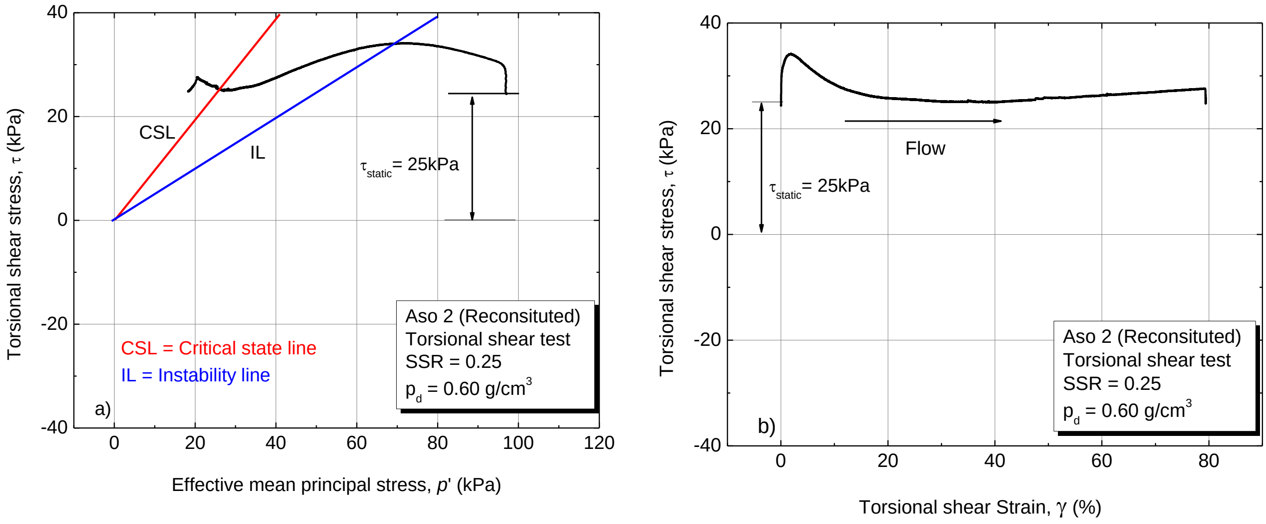

Figure 11. Torsional shear test ASO #2: a) effective stress path; and b) stress strain relationship

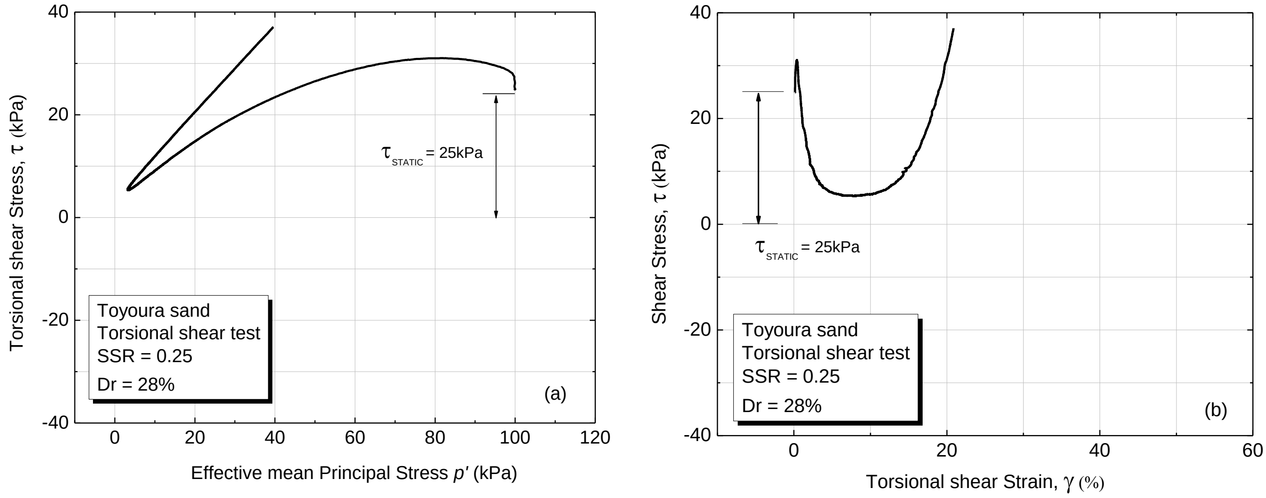

Figure 12. Torsional shear behavior of Toyoura sand: a) effective stress path; and b) stress strain relationship

3.5 Specimen deformation under torsional shear loading

The deformation characteristics of Aso pumice specimen at various stage of shearing in undrained torsional shear test (Test ASO #3) are shown in Figure 13. At stage , corresponding to a shear strain (γ) of about 7.5 %, the deformation was uniform throughout the specimen height. At stage 3 (γ = 15 %), the deformation was still rather uniform. However, at stage 4 (γ = 30 %), it appears that strain localization started to develop in the upper part of the specimen.

A similar deformation pattern was reported by Kiyota et al. (2008), Chiaro et al. (2012) and Umar et al. (2016) also for the case of Toyoura sand. However, in the case of Aso pumice, the specimen deformation and shape remain rather uniform even at high shear strain of 30%. This difference in specimen deformation and strain localization near top cap between Toyoura sand and Aso pumice can be attributed to migration of water to the surface (i.e. water film formation) in the case of Toyoura sand specimen.

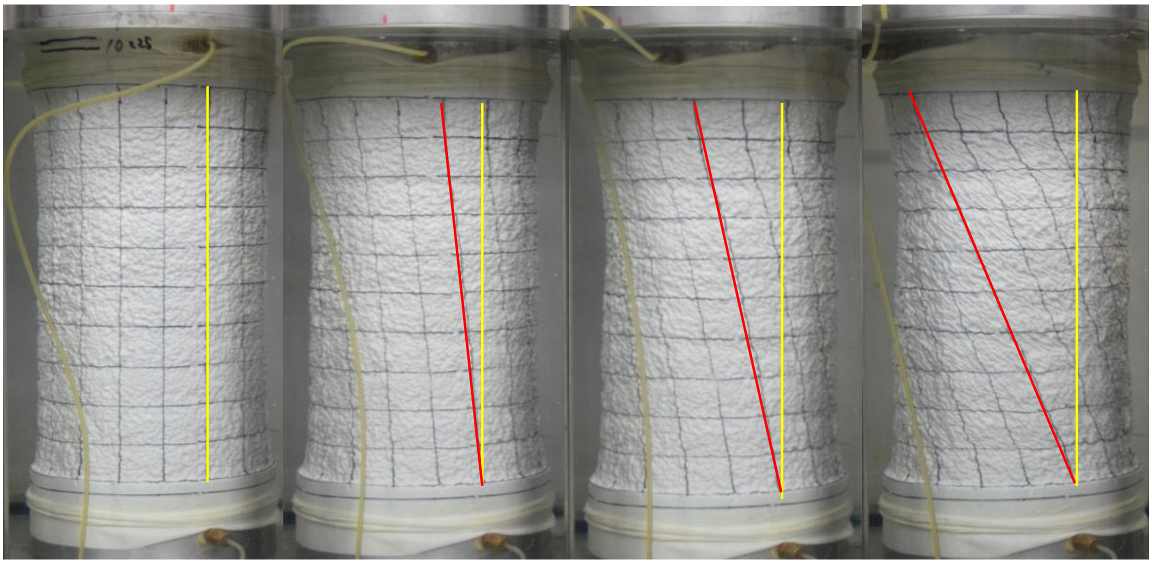

Stage 1 (γ = 0%) Stage 2 (γ = 7.5%) Stage 3 (γ = 15%) Stage 4 (γ = 30%)

Figure 13. Typical deformation of Aso pumice specimens in cyclic undrained torsional shear tests

4. CONCLUSIONS

In this paper, an attempt was made to clarify the behavior of undisturbed and reconstituted specimens of Aso pumice soil under undrained monotonic and cyclic loading conditions using torsional and triaxial apparatuses, respectively. The test results revealed that, Aso pumice soil has the tendency to show flow-type failure behavior characterized by an abrupt development of large shear strains. It was noticed that pumice soil exhibits different behavior as compared to that of Toyoura sand, and state of liquefaction (p_0*'=0*) was not reached in pumice soil. On the contrary, under cyclic shear stress condition triaxial and torsional shows a different trend of development of pore water pressure. In torsional simple shear, a progressive build-up of excess pore water pressure was observed until the stress state reached the failure envelop. It was followed by a flow-type failure with a rapid development of large shear strains. In addition, Takanodai landslide was simulated with the same stress condition as insitu and it is found that large deformation resulted in exceeding the peak undrained resistance, and reach a critical state line, where progressive flow failure continue to develop up to extremely large deformation.

5. REFERENCES

Ampadu SIK (1991). Undrained behavior of kaolin in torsional simple shear, *Ph.D. Thesis*, Dept. of Civil Engineering, University of Tokyo, Japan.

Chiaro G, Koseki J, Sato T (2012). Effects of initial static shear on liquefaction and large deformation properties of loose saturated Toyoura sand in undrained cyclic torsional shear tests, *Soil and Foundations*, 52(3): 498–510.

Chiaro G, Koseki J, De Silva LIN (2013). A density- and stress-dependent elasto-plastic model for sands subjected to monotonic torsional shear loading, *SEAGS Geotechnical Engineering Journal*, 44(2): 18-26.

Chiaro G, Kiyota T, Miyamoto H (2015). Large deformation properties of reconstituted Christchurch sand subjected to undrained cyclic torsional simple shear loading, *Proc. of the NZSEE Annual Technical Conference*, Apr. 10-12, Rotorua, New Zealand, 529-536.

Chiaro G, Alexander G, Brabhaharan P, Massey C, Koseki J, Yamada S, Aoyagi Y (2017). Reconnaissance report on geotechnical and geological aspects of the 2016 Kumamoto Earthquake, Japan, *Bulletin of the New Zealand Society for Earthquake Engineering*, 50(3): 365-393.

Dang K, Sassa K, Fukuoka H, Sakai N, Sato Y, Takara K, Quang LH, Loi DH, Tien PV, Ha, ND (2016). Mechanism of two rapid and long runout landslides in the 16 April 2016 Kumamoto earthquake using a ring-shear apparatus and computer simulation (LS-RAPID), *Landslides*, 13(6): 1525–1534.

Goto S, Tatsuoka F, Shibuya S, Kim YS, SatoT (1991). A simple gauge for local small strain measurements in the laboratory, *Soils and Foundations*, 31(1), 169-180.

Hyodo M, Hyde AFL, Aramaki, N (1998). Liquefaction of crushable soils, *Geotechnique*, 48(4): 527-543.

Kiyota T, Sato T, Koseki J, Mohammad A (2008). Behavior of liquefied sands under extremely large strain levels in cyclic torsional shear tests, *Soils and Foundations*, 48(5), 727-739.

Liu L, Orense RP, Pender MJ (2015). Crushing induced liquefaction characteristic of Pumice sand, *Proc. of the NZSEE Annual Technical Conference*, Apr. 10-12, Rotorua, New Zealand.

Mukunoki T, Kasama T, Murakami S, Ikemi H, Ishikura R, Fujikawa T, Yasufuka N, Kitazono Y (2016). Reconnaissance report on geotechnical damage caused by an earthquake with JMA seismic intensity 7 twice in 28h, Kumamoto, Japan. *Soils and Foundation*, 56(6): 947-964.

Orense RP, Pender MJ (2016). From micro to macro : An investigation of the geotechnical properties of pumic sand, *Proceeding of the International Workshop on Volcanic Rocks and Soils*, Ischia Island, Italy, 24-25 Sept 2016.

Pender MJ, Wesley LD, Larkin TJ, Pranjoto S (2006). Geotechnical properties of a pumice sand, *Soil and Foundations*, 46(1), 69-81.

Wesley LD, Meyer VM, Pranjoto S, Pender MJ, Larkin TJ, Duske GC (1999): Engineering properties of pumice sand, *Proc. of the 8th Australia-NZ Conference on 'Geomechanics'*, Hobart, TAS, **2**: 901–908.

Umar M, Chiaro G, Kiyota T (2016). On the influence of initial static shear on large deformation behavior of very loose Toyoura sand in undrained cyclic torsional shear tests, *JGS Special Publication*, 4: 17-22.